Characterization of Rhodopsin–Transducin Interaction: A Mutant Rhodopsin Photoproduct with a Protonated Schiff Base Activates Transducin†

Tatyana A. Zvyaga, Karim Fahmy, and Thomas P. Sakmar*

The Howard Hughes Medical Institute, Laboratory of Molecular Biology and Biochemistry, Rockefeller University, New York, New York 10021

Received January 19, 1994; Revised Manuscript Received April 21, 1994®

ABSTRACT: Rhodopsin, a G protein-coupled seven-transmembrane helix receptor, contains an 11-*cis*-retinal chromophore covalently linked to opsin apoprotein by a protonated Schiff base. Photoisomerization of the chromophore followed by Schiff base deprotonation forms metarhodopsin II (MII, λ_{max} = 380 nm), the active state (R*) that catalyzes guanine nucleotide exchange in transducin, the G protein of the photoreceptor cell. Schiff base deprotonation is required for R* formation. The Schiff base positive charge in rhodopsin is stabilized by a carboxylic acid counterion, Glu^{113}. The position of the carboxylate counterion was moved by one helix turn to position 117 by site-specific mutagenesis. Photolysis of the mutant pigment E113A/A117E (λ_{max} = 491 nm) resulted in a mixture of two photoproducts: (1) an MII-like form with an unprotonated Schiff base (λ_{max} = 382 nm) favored at alkaline pH; and (2) a photoproduct with a protonated Schiff base (λ_{max} = 474 nm), spectroscopically similar to metarhodopsin I, favored at acidic pH. Here, we have studied the interactions between the mutant E113A/A117E photoproducts and transducin in detail. Transducin slowed down thermal conversion of the 474 nm form to the 382 nm form by stabilizing the 474 nm photoproduct. This effect was maximal at the pH optimum of transducin activation by the mutant R* and was abolished in the presence of GTPγS. In addition, the amount of the 474 nm species correlated with transducin activation rates during the thermal conversion of the photoproduct mixture. Thus, the 474 nm photoproduct of the mutant pigment, which contained a protonated Schiff base, activated transducin. The results suggest that net Schiff base deprotonation in rhodopsin is not an essential determinant of the R* conformation *per se*, but may be required for neutralization of the carboxylic acid counterion.

Rhodopsin, the visual photoreceptor of the rod cell, is a member of the superfamily of seven-transmembrane helix receptors that activate guanine nucleotide-binding regulatory proteins (G proteins).[1] It contains an 11-*cis*-retinal chromophore that is covalently linked by a protonated Schiff base to Lys^{296} of the opsin apoprotein (Bownds, 1967; Dratz & Hargrave, 1983; Oseroff & Callendar, 1974). Photoisomerization of the chromophore to the all-trans form results in a series of spectrally defined intermediates (Yoshizawa & Shichida, 1982). During the transition of metarhodopsin I (MI, λ_{max} = 470 nm) to metarhodopsin II (MII, λ_{max} = 380 nm), the Schiff base becomes deprotonated (Doukas et al., 1978; Mathews et al., 1963). MII has been identified as the active receptor conformation, R*, which catalyzes guanine nucleotide exchange by the G protein transducin (Kibelbek et al., 1991). Chemical modification of rhodopsin has demonstrated that transducin activation is abolished if Schiff base deprotonation is prevented (Longstaff et al., 1986). Obviously, the Schiff base protonation state plays a crucial role for receptor–G protein coupling in this system, and Schiff base deprotonation is considered a prerequisite for receptor activation. Correspondingly, amino acid side chains which stabilize or destabilize the positive charge at the Schiff base nitrogen in rhodopsin and its MII photoproduct, respectively, may be important to switch from an inactive to an active receptor conformation after chromophore photoisomerization.

Site-specific mutagenesis studies have identified Glu^{113} as the counterion to the protonated retinylidene Schiff base in dark rhodopsin (Lin et al., 1992; Nathans, 1990; Sakmar et al., 1989; Zhukovsky & Oprian, 1989). The predominant effect of replacement of Glu^{113} by a neutral amino acid residue such as glutamine or alanine was a lowering of the Schiff base acidity constant (pK_a) to about 6. Two reports have described the effect of moving the position of the Schiff base counterion by one helix turn in the third transmembrane domain of rhodopsin (Zhukovsky et al., 1992; Zvyaga et al., 1993). A carboxylic acid residue at position 117 could functionally replace Glu^{113} to yield a pigment with a visible-absorbing λ_{max} and an apparently normal pK_a in the dark state. In addition, the mutant pigments could activate transducin in response to light.

Here, the interactions between the mutant E113A/A117E photoproducts and transducin are studied in detail. Illumination of the detergent-solubilized mutant E113A/A117E produced a mixture of photoproducts composed of a 382 nm absorbing species having an unprotonated Schiff base and a 474 nm absorbing form containing a protonated Schiff base. However, the pH dependency of the 474 nm/382 nm mutant photoproduct equilibrium was altered as compared to the MI/MII equilibrium in rhodopsin (Hofmann, 1986; Mathews et al., 1963; Parkes & Liebman, 1984). Acidic pH favored the 474 nm form, and basic pH favored the 382 nm form of the mutant photoproduct. Therefore, the 474 nm form of the E113A/A117E photoproduct may be formed differently from MI of rhodopsin or the MI-like states favored in other rhodopsin mutants (Weitz & Nathans, 1993).

† T.P.S. is an Assistant Investigator, and T.A.Z. and K.F. are Associates of the Howard Hughes Medical Institute.

* Address correspondence to this author at Box 284, Rockefeller University, 1230 York Ave., New York, NY 10021. Telephone: 212-327-8288. FAX: 212-327-8370.

® Abstract published in *Advance ACS Abstracts,* July 15, 1994.

[1] Abbreviations: DTT, dithiothreitol; G protein, guanine nucleotide-binding regulatory protein; MI, metarhodopsin I; MII, metarhodopsin II; MOPS, 3-(*N*-morpholino)propanesulfonic acid, R*, photoactivated rhodopsin; T_α, α-subunit of transducin; UV, ultraviolet.

0006-2960/94/0433-9753$04.50/0

In this report, we show that despite the pronounced pH dependence of the mutant photobleaching behavior, no corresponding shift in the pH sensitivity of transducin activation was observed when compared with detergent-solubilized rhodopsin in a fluorescence assay. However, the presence of transducin slowed the thermal conversion of the mutant 474 nm photoproduct to the 382 nm photoproduct. This effect was abolished by the addition of the GTP analog GTPγS, indicating that functional complexes had formed. Furthermore, the thermal transition of the 474 nm photoproduct to the 382 nm photoproduct correlated directly to a decrease of the ability of the mutant pigment to activate transducin. Thus, light-dependent transducin activation could be accounted for only by an "active" 474 nm photoproduct. These results show that the mutations produced an R* conformation that contained a protonated Schiff base chromophore–opsin linkage. Consequently, a neutral Schiff base may not be strictly required in photoactivated vertebrate visual pigments. The results argue that in native rhodopsin, deprotonation of the Schiff base may be required to neutralize the counterion at position 113. Schiff base deprotonation may not be essential for R* formation if the counterion residue is neutralized by other means.

MATERIALS AND METHODS

Materials. Sources of most materials have been previously reported (Franke et al., 1992; Sakmar et al., 1989, 1991). Dodecyl maltoside detergent was purchased from Anatrace, Inc. (Cleveland, OH). Radionucleotides were from Du Pont–New England Nuclear, and BA85 nitrocellulose filters were from Schleicher & Schuell. Nucleotides were purchased from Boehringer Mannheim.

Preparation of Rhodopsin Mutant. The opsin mutant E113A/A117E was prepared by cassette mutagenesis of a synthetic gene for bovine rhodopsin (Ferretti et al., 1986) that had been cloned into the expression vector as previously described (Franke et al., 1988). Opsin genes were expressed in COS-1 cells following transient transfection by a DEAE-dextran procedure as described (Oprian et al., 1987). COS cells expressing the mutant apoproteins were harvested and then incubated in the presence of 11-*cis*-retinal under dim red light to reconstitute pigments as described (Franke et al., 1992; Sakmar et al., 1989). The purification procedure employed was based on the immunoaffinity procedure of Oprian et al. (1987) that was modified as described (Franke et al., 1992; Karnik et al., 1988; Sakmar et al., 1989). Pigments were generally prepared in 100 mM NaCl/0.1% dodecyl maltoside detergent and concentrated using Centricon-30 membrane filters (Amicon) to final pigment concentrations of about 10 μM ($A_{500} \approx 0.5$ cm^{-1}). In order to carry out experiments at different pH values, concentrated buffer solutions (10×) were added to give the desired final pH value. The pigments described in this report were prepared exclusively from COS cells.

UV–Visible Absorption Spectroscopy. Spectroscopy was performed on a λ-19 Perkin-Elmer spectrophotometer at 15 °C on purified detergent-solubilized samples in a cuvette with a 1-cm path length (Chan et al., 1992). All pigment samples (≈1 μM) were studied in solutions of 50 mM Tris–maleate (pH 6–8), 100 mM NaCl, 2 mM $MgCl_2$, 1 mM DTT, and 0.01% dodecyl maltoside detergent. The pigment spectra in Figure 5, 6A, and 7A are presented without alteration of data by averaging or smoothing algorithms. Other spectra are displayed after smoothing using the Perkin-Elmer uvcss data handling software package.

A simple computer algorithm was used to determine the relative amount of 474 nm photoproduct in samples that contained a mixture of several spectral forms. For a given set of conditions, a spectrum of the pure 474 nm absorbing species was initially recorded. At the end of an experiment after thermal decay of the 474 nm form had occurred, a final spectrum was recorded. Any intermediate spectrum could be defined in terms of a relative sum of the initial and final spectra of a thermal decay experiment. The same algorithm was applied for the determination of the composition of a mixture of free *all-trans*-retinal and protonated Schiff base after acid denaturation of pigment (see below).

Photolysis of Mutant Rhodopsin Pigments. Samples were illuminated directly in the spectrophotometer cuvette using a fiber-optic light guide (Dolan-Jenner, Inc.) connected to a light source (150-W projector lamp) fitted with a 495 nm long-pass filter (Oriel, Inc.). Illumination times were precisely controlled using an electronic shutter built into the fiber-optic light guide (Melles-Griot). Photolysis was carried out at 15 °C unless otherwise noted. All pigment samples (≈1 μM) were studied in the presence or absence of purified transducin (3 μM), and GTPγS (5 μM) depending upon the particular experiment. Transducin storage buffer (see below) was added to samples in the absence of transducin in order to match buffer conditions.

Fluorescence Assay of Transducin Activation Rates. Bovine transducin was purified from rod outer segment extracts by hexylagarose chromatography and preloaded with GDP (Fung et al., 1981). Transducin was stored at −20 °C in 10 mM MOPS, pH 7.5, 2 mM $MgCl_2$, 1 mM DTT, 5 μM GDP, and 50% glycerol. Fluorescence assays of transducin activation by rhodopsin and the mutant pigment as a function of pH at various nucleotide concentrations were carried out as previously described (Fahmy & Sakmar, 1993a). Essentially, a mixture of transducin and rhodopsin (10 mM Tris–maleate, 100 mM NaCl, 2 mM $MgCl_2$, 1 mM DTT, and 0.01% dodecyl maltoside) was photoactivated in the spectrofluorometer. The sample was excited at 300 nm, and fluorescence was recorded at 345 nm. After 5 min, GTPγS was injected into the cuvette, and the fluorescence increase at 345 nm was recorded. A linear regression was applied to the data points which corresponded to a fluorescence increase of 30% of the maximal fluorescence signal. The slope of the regression line was taken as a relative measure of the transducin activation rate. We estimate an error of ±8% in the values for relative rates based on reproducibility of recordings from independent experiments on identical samples.

Transducin Activation Assay and Measurement of Activity Decay Rates. A radionucleotide filter-binding assay, which monitors the light-dependent guanine nucleotide exchange by transducin, was carried out as previously described (Wessling-Resnick & Johnson, 1987) except as noted below. The assay mixture (final volume of 0.1 mL) consisted of purified pigment (10 nM), purified transducin (0.01 mL, ≈3 μM), and [^{35}S]GTPγS (20 μM) in assay buffer (50 mM Tris–maleate, pH 7.0 or 8.0, 100 mM NaCl, 2 mM $MgCl_2$, 1 mM DTT, and 0.01% dodecyl maltoside). The time course of activity decay after illumination of the mutant pigment in the absence of transducin was measured. Aliquots were removed over time and diluted with a GTPγS-containing buffer to give the assay conditions described above. The pigment aliquots were mixed with GTPγS before addition to the transducin solution in order to avoid any changes in the composition of the photoproduct mixture that might be caused by transducin binding. This allowed a direct correlation with the spectro-

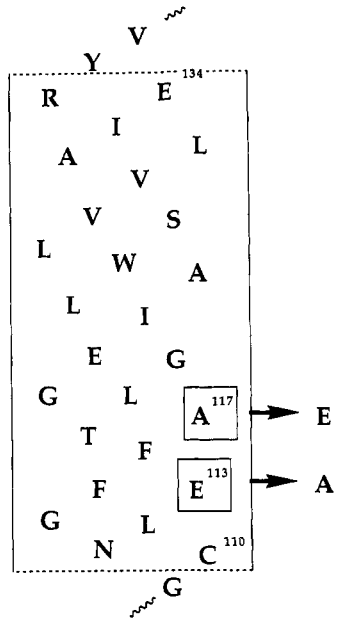

FIGURE 1: Schematic representation of the third transmembrane helix (helix C) in bovine rhodopsin. Amino acids replaced in putative helix C are boxed and numbered. The mutant described in this report is the double-replacement mutant E113A/A117E. Cys^{110} has been reported to form a disulfide bond with Cys^{187} and may form the intradiscal border of helix C (Karnik et al., 1988). The charged pair Glu^{134}/Arg^{135} has been shown to be involved in transducin interaction (Sakmar et al., 1989). The helical secondary structure of this domain is supported by additional mutagensis experiments (Zhukovsky et al., 1992).

scopic data measured in the absence of transducin. This protocol also controlled for noncatalytic nucleotide exchange since the time during which GTPγS was incubated with transducin was identical for each aliquot even though different times had elapsed since photolysis. Transducin activation rates were determined by linear regression analysis of the increasing amount of radioactivity retained on successive filters. A control experiment was also performed to show whether or not the mutant opsin was constitutively active. The mutant showed no constitutive activity under the conditions of the assay employed.

Measurement of Schiff Base Hydrolysis Rates. An acid denaturation method was used to monitor the rate of Schiff base hydrolysis after illumination. Under acidic conditions, rhodopsin denatures, but the chromophore–opsin Schiff base linkage is stable and results in a broad peak with λ_{max} of 440 nm. Free *all-trans*-retinal gives a peak with λ_{max} of about 385 nm. The relative contributions of these two peaks to the spectrum obtained after acid addition are directly proportional to the amount of Schiff base present. Experiments were carried out at 15 °C. After an initial dark spectrum was recorded on a 90 μL aliquot, the remaining sample was illuminated for 5 s. After defined decay times, 10 μL of 2 M hydrochloric acid was added to aliquots to denature the pigment, and spectra were recorded.

RESULTS

Preparation and Spectroscopic Characterization of Mutant Pigment. A double amino acid replacement mutant was prepared (E113A/A117E) to reposition the carboxylate Schiff base counterion by one helix turn within helix C as shown in Figure 1. The mutant gene was expressed in a monkey kidney cell line (COS-1) (Oprian et al., 1987). The expressed mutant opsin was regenerated with 11-*cis*-retinal and purified by an immunoaffinity absorption procedure (Franke et al., 1992;

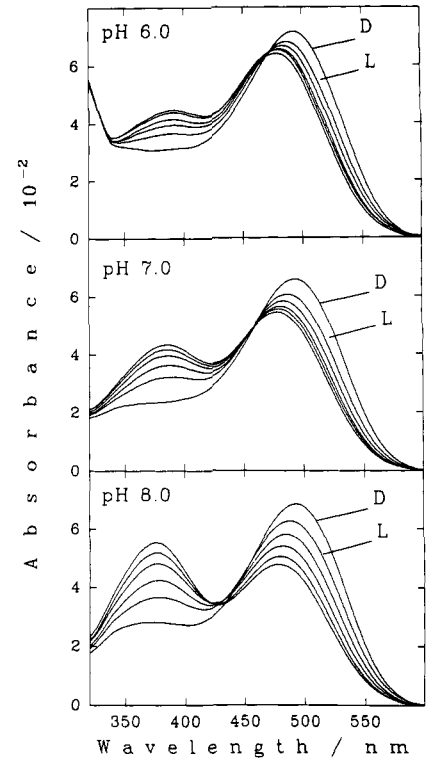

FIGURE 2: Effect of pH on the photolysis of mutant pigment E113A/A117E. Pigment samples regenerated with 11-*cis*-retinal were prepared at three pH values: 6.0, 7.0, and 8.0. A dark spectrum was recorded for each sample (D) at 1 °C. Each sample was then illuminated with five successive 1 s flashes. The spectra resulting from the first flash are labeled (L). Subsequent spectra are superimposed. Spectra were recorded during 1 min intervals between flashes. At acidic pH, photolysis results predominantly in a 474 nm absorbing photoproduct with a small component absorbing at 382 nm. At basic pH, the predominant photoproduct absorbed at 382 nm. Acid denaturation of each photolyzed sample at the conclusion of the experiment resulted in a 440 nm absorbing species (not shown) and indicated that the Schiff base linkage was intact.

Oprian et al., 1987; Sakmar et al., 1989). The mutant opsin bound 11-*cis*-retinal to form a visible chromophore absorbing with a λ_{max} value of 491.3 ± 0.2 nm (mean ± standard error, n = 18). The detergent-solubilized mutant displayed photobleaching properties different from those of recombinant rhodopsin. Photolysis of rhodopsin in dodecyl maltoside detergent resulted in complete photoconversion to MII (λ_{max} ≈ 380 nm). Photolysis of the mutant produced a pH-dependent mixture of photoproducts absorbing at 473.7 ± 0.7 nm (n = 28) and 381.6 ± 1.0 nm (n = 34). The effect of pH on photolysis of the mutant pigment was evaluated. Pigment samples were prepared at pH values 6.0, 7.0, and 8.0. The mutant pigment was subjected to successive flashes of light followed by UV–visible spectroscopy as shown in Figure 2. At acidic pH, photolysis resulted predominantly in a 474 nm absorbing photoproduct with a small component absorbing at 382 nm. At basic pH, the predominant photoproduct absorbed at 382 nm. Acid denaturation of each photolyzed sample at the conclusion of the experiment resulted in a 440 nm absorbing species (not shown) and indicated that the Schiff base linkage remained intact.

Interaction between Mutant E113A/A117E Photoproducts and Transducin. In order to clarify which of the photoproducts was responsible for transducin activation, experiments were designed to take advantage of conditions which favored one or the other of the mutant photoproducts. Comparing the amounts of the 382 nm and 474 nm forms to the rates of transducin activation measured under the same conditions

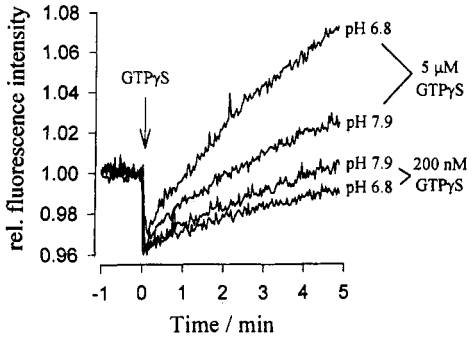

FIGURE 3: Fluorescence time course of transducin activation by mutant E113A/A117E. Superimposed fluorescence traces of transducin activation are shown for two different pH values (6.8 and 7.9) and two different concentrations of GTPγS (5 μM and 200 nM). The reactions were started (arrow) by the addition of GTPγS (to the final concentrations indicated) to a mixture of light-activated pigment (0.9 nM) and transducin (240 nM) in detergent (0.01% dodecyl maltoside) buffer. Experiments were carried out under continuous illumination at 10 °C. With 200 nM GTPγS, where nucleotide exchange was rate-limiting, the effect of pH on the rate of fluorescence increase was reversed as compared to the reaction in the presence of 5 μM GTPγS, where complex formation was rate-limiting.

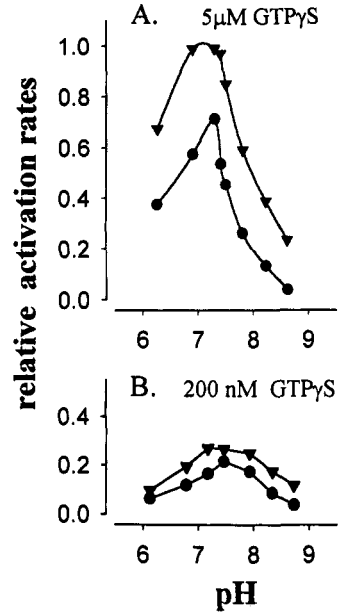

FIGURE 4: Mutational effects on the pH dependence of relative activation rates at different concentrations of GTPγS. The pH dependence of relative activation rates was measured for rhodopsin (triangles) and mutant E113A/A117E (circles) at 5 μM (A) and 200 nM (B) GTPγS concentrations. (A) The formation rate of R*–transducin complexes determined the rise of T_α(GTPγS) fluorescence. (B) Complexes could accumulate, and correspondingly the complex dissociation rates determined the transducin activation rate (Fahmy & Sakmar, 1993a). Each point was determined from a fluorescence time course as shown in Figure 3 using Tris–maleate buffers of varying pH. The ordinate is scaled so that the maximum activation rate of rhodopsin (at pH 7) equals 1. Measuring conditions were as described in the legend to Figure 3. In individual rate determinations, the error is estimated to be ±8%.

should allow assessment of the ability of each photoproduct to activate transducin. Three types of experiments were carried out. First, since pH affected the proportion of photoactivated pigment absorbing at 474 nm versus 382 nm, the transducin activation rate of the photoactivated mutant was measured as a function of pH and compared to that of rhodopsin. In a second set of experiments, the effect of transducin on the thermal transition of the 474 nm form to the 382 nm form of the mutant photoproduct was studied as a function of pH in the presence and absence of GTPγS. Finally, transducin activation rates were correlated with the relative amounts of 382 nm and 474 nm absorbing mutant photoproducts.

(a) pH Dependence of E113A/A117E–Transducin Complex Formation Rate and Nucleotide Exchange Rate. Transducin activation rates were determined in a fluorescence assay based on the increase of intrinsic Trp^{207} fluorescence of the α-subunit of transducin upon GTPγS binding (Faurobert et al., 1993) as described previously (Fahmy & Sakmar, 1993a). The time course of the fluorescence recording was started upon addition of GTPγS to a mixture of photobleached pigment and transducin. Figure 3 shows four selected traces obtained at two different pH values and two different concentrations of GTPγS. The effect of pH on the measured rates depended on the amount of GTPγS added to start the reaction. When the nucleotide was present in excess (5 μM), a drop in transducin activation was observed upon increasing the pH from 6.8 to 7.9. When the GTPγS concentration was reduced to 200 nM, a faster rate was obtained at pH 7.9 as compared to pH 6.8. This relative enhancement of activation rates at alkaline pH and low nucleotide concentration has been observed with all recombinant pigments studied so far in this manner (Fahmy & Sakmar, 1993a). It has been attributed to a difference in the pH dependence of R*–transducin complex formation, which determines the overall reaction rate at high GTPγS concentrations, as compared to the pH dependence of the subsequent nucleotide exchange reaction in transducin, which limits the reaction rate at low GTPγS concentrations. The mutant pigment was tested under both conditions in order to detect deviations in the pH profiles of either of the specific reaction rates from those obtained with rhodopsin.

Figure 4A shows a comparison of the pH profiles obtained for E113A/A117E to those from recombinant rhodopsin using the same transducin preparation. The data points were obtained by plotting the slope of regression lines through fluorescence traces between zero time and the time corresponding to 30% of the final fluorescence increase. Values were normalized to the maximal activation rate by R* in the presence of 5 μM GTPγS. The pH optimum for rhodopsin binding to transducin was 7. This finding agrees with a previous determination of the pH optimum for the R*–transducin complex formation rate, which drops by approximately 50% within 1 pH unit to either side of the optimum (Fahmy & Sakmar, 1993a). The E113A/A117E–transducin interaction differed from the rhodopsin–transducin interaction in two ways. First, the E113A/A117E–transducin complex formation rate was ≈30% slower than that of rhodopsin. Second, the pH-dependence curve was steeper on both sides of the optimal pH. Interestingly, the pH optimum of the mutant did not differ significantly from that of rhodopsin (pH 7). Thus, the difference in the proportion of 382 nm to 474 nm photoproducts as a function of pH was not reflected in the pH dependence of mutant R*–transducin complex formation rates.

Similarly, when assayed at 200 nM GTPγS, where the nucleotide exchange reaction was rate-limiting, mutant E113A/A117E and rhodopsin displayed the same pH profiles (Figure 4B). For each pigment, the relative enhancement of this reaction step at alkaline pH demonstrated above (Figure 3) was manifested as a broadening of the curve toward alkaline pH when compared to the curves assayed at high GTPγS concentration (5 μM). In spite of the significant effect of the mutation on the Schiff base environment in the mutant photoproduct, neither the pH sensitivity of the association of

mutant R* with transducin nor the nucleotide-dependent complex dissociation was affected.

The similar pH dependence of complex formation rates and nucleotide exchange rates obtained with R* and mutant R* does not suggest that transducin interacts exclusively with one of the two mutant photoproducts. However, the intrinsic pH dependencies of transducin activation by the two mutant photoproducts cannot be measured because of the pH-dependent shift in the E113A/A117E photoproduct mixture (Figure 2). Therefore, a preference of transducin to interact with one spectral form or the other may have been offset by the unknown pH effect on the activation rate of a particular form. For this reason, experiments were designed where the relative amounts of the mutant photoproducts could be varied without simultaneously varying the pH.

(b) Effect of Transducin on the Rate of Thermal Reactions of E113A/A117E Photoproducts at Different pH Values. The binding of transducin to R* causes a stabilization of the active state and a slower rate of Schiff base hydrolysis (Bennett et al., 1982; Bruckert et al., 1992; Emeis et al., 1982). Both effects are abolished by the addition of GTPγS, which induces the dissociation of R*–transducin complexes and thus removes the stabilizing effect of transducin. In the case of the mutant E113A/A117E, a preference for transducin binding to a particular photoproduct form may be displayed as a selective stabilization of this species over a noninteracting form. Therefore, the thermal reactions of the mutant photoproducts were monitored by UV–visible spectroscopy in the presence and absence of transducin and/or GTPγS. Figure 5 shows the spectral changes in the photoproduct mixture in the absence of transducin, in the presence of transducin (3 μM), and in the presence of both transducin (3 μM) and GTPγS (5 μM). These experiments were carried out at three different pH values. At any pH value, transducin slowed down the transition of the 474 nm absorbing form to the 382 nm absorbing form. This can be quantitated by comparing the 474 nm absorption change over 10 min in the presence of transducin (+T, –GTPγS), or in the presence of both transducin and GTPγS (+T, +GTPγS), to the 474 nm absorption change observed in the absence of both substances. Results from several experiments are summarized in Table 1. In the presence of transducin at three pH values tested, the 474 nm absorption decrease over 10 min was smaller than that in the absence of transducin. The addition of GTPγS abolished this effect of transducin and allowed decay of the 474 nm photoproduct of similar magnitude as observed with the photoproduct mixture alone. The stabilizing effect of transducin on the 474 nm form was largest at pH 7, the pH optimum for mutant R*–transducin complex formation (Figure 4A). Therefore, the formation of functional complexes capable of undergoing GTPγS-induced dissociation may be also responsible for the stabilizing effect of transducin on the 474 nm photoproduct. This agrees with the fact that at all pH values, the addition of GTPγS abolished the stabilization of the 474 nm photoproduct.

Since the pigment may decay to opsin plus free *all-trans*-retinal during the course of these experiments, which contributes to the 382 nm absorbance, the slower decay of the 474 nm absorbance in the presence of transducin does not necessarily mean that this species becomes relatively enriched versus the 382 nm form. However, at pH 8 the Schiff base decay in the absence of transducin was found to be slow as compared to the time scale on which the 474 nm to 382 nm absorbance change occurred (see below). This implies that the 382 nm absorbance was almost entirely due to the 382 nm

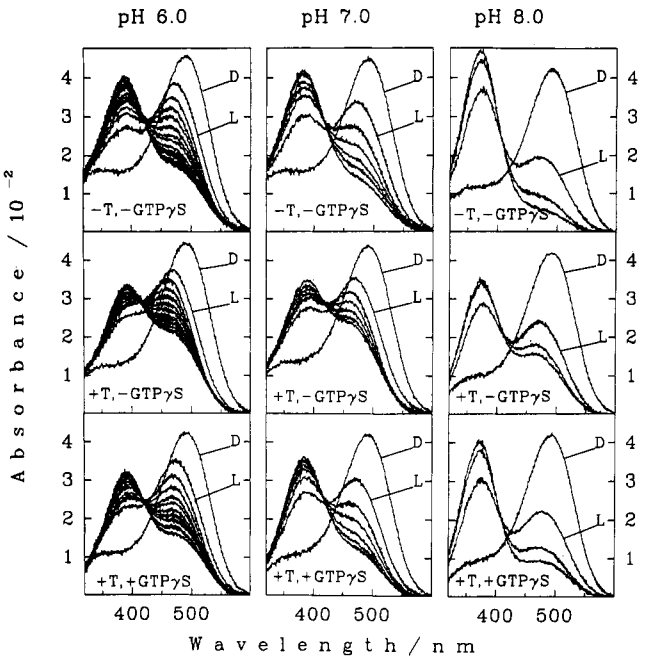

FIGURE 5: Effect of transducin on the rates of thermal reactions of mutant pigment E113A/A117E photoproducts at different pH values. The experiment was designed to monitor the effect of transducin on the thermal conversion of the 474 nm absorbing photoproduct to the 382 nm species. Mutant pigment samples were prepared at pH 6.0, 7.0, and 8.0. Three experiments are shown for each pH value: (1) –transducin, –GTPγS; (2) +transducin, –GTPγS; (3) +transducin, + GTPγS. A dark spectrum was recorded for each sample (D). Photolysis was then carried out with a 5 s flash (L). Each mixture was then incubated in the cuvette in the dark at 15 °C, and spectra were recorded. In each panel, spectra corresponding to time intervals of 5 min are superimposed. At each pH value, the 474 nm absorbing photoproduct converts over time to a 382 nm species. The rate of conversion is fastest at pH 8.0 and slowest at pH 6.0. The 382 nm absorbing peak under these conditions corresponds to a mixture of an MII-like species containing a Schiff base linkage, and free *all-trans*-retinal plus mutant opsin. At pH 7.0, the rate of conversion from the 474 nm peak to the 382 nm peak is retarded by the presence of transducin without GTPγS (pH 7.0, middle panel). The rate of conversion in the presence of transducin plus GTPγS (pH 7.0, lower panel) is very similar to the rate in the absence of transducin (pH 7.0, upper panel). Even though the intrinsic rate of conversion of the 474 nm peak to the 382 nm peak is faster at pH 8.0, the same effect of 474 nm species stabilization in the presence of transducin minus GTPγS is observed. This can be appreciated by comparing the –transducin, –GTPγS conditions (pH 8.0, upper panel) and +transducin, +GTPγS conditions (pH 8.0, lower panel) to the +transducin, –GTPγS conditions (pH 8.0, middle panel). The effect is slightly less pronounced at pH 8.0 as compared to the effect at pH 7.0. There is also an obvious effect of transducin on the conversion of the 474 nm species at pH 6.0 where the formation of the 382 nm species is the slowest among the three pH values tested. A summary of results is presented in Table 1.

photoproduct, which contained an unprotonated Schiff base. Therefore, the above experiments carried out at pH 8 strongly suggest that transducin enriched the photoproduct mixture in favor of the 474 nm form.

In these experiments, photolysis was carried out by successive 1-s flashes until complete photoconversion was achieved (five flashes). The spectrum labeled L in each panel of Figure 5 contained no residual dark pigment and was recorded 5 min after the initial flash. Thus, the larger amount of 474 nm form in the presence of transducin is due to the stabilizing effect of transducin during the initial 5 min of the experiment rather than to a difference in the initial amount of 474 nm species formed by photolysis. The photobleaching difference spectra after 1 s illumination are virtually identical in the presence or absence of transducin (data not shown). Therefore,

Table 1: Thermal Decay of the 474 nm Photoproduct in the Presence of Transducin and GTPγS[a]

	ΔA_{474} (%)		
	pH 6	pH 7	pH 8
–T, –GTPγS	100	100	100
+T, –GTPγS	82	56	62
+T, +GTPγS	108	92	93

[a] The absorption decrease at 474 nm (ΔA_{474}) observed over 10 min in the presence of transducin alone (+T, –GTPγS) and in the presence of both transducin and GTPγS (+T, +GTPγS) is expressed as a percentage of the absorption change over 10 min in the presence of buffer only (–T, –GTPγS), which is defined as 100%. Data are taken from experiments as presented in Figure 5. For pH 6 and pH 7, the values are averages of three time intervals of 10 min each.

association of the mutant photoproduct(s) with transducin did not seem to increase the initial amount of 474 nm photoproduct at the expense of the 382 nm form. The effect of transducin was apparent only on the time scale of the thermal decay reactions. Likewise, GTPγS-induced dissociation of transducin from the stabilized mutant R*–transducin complex did not cause an immediate change in the 474 nm and 382 nm absorbance (not shown). Both observations argue against a transducin-dependent equilibration between the 474 nm and the 382 nm forms of the mutant photoproduct on a time scale which is faster than that of the thermal transition. Therefore, the stabilization of the 474 nm species was most likely caused by binding of transducin to the 474 nm form rather than by a transducin-induced back-conversion of the 382 nm species to the 474 nm photoproduct.

(*c*) *Correlation of Transducin Activation Rates with the Relative Amounts of 382 nm and 474 nm Absorbing Mutant Photoproducts.* The experiments described above indicated that transducin bound to the 474 nm photoproduct and slowed down its thermal conversion to the 382 nm form. Since rhodopsin mutants have been described that bound but did not activate transducin (Franke et al., 1990), it may be that the 474 nm mutant photoproduct bound transducin but that the activity measured in the fluorescence assay (Figure 3) was exclusively due to the 382 nm species. However, the abolishment of transducin-dependent stabilization of the 474 nm species by addition of GTPγS suggested that this mutant photoproduct catalytically activated transducin. This hypothesis was tested in the experiments described below.

The slow thermal and pH-dependent transition of the 474 nm form to the 382 nm form after photoactivation of the mutant (Figure 5) was exploited to obtain photoproduct mixtures with different relative amounts of the two potential mutant R* forms. A solution of dark mutant pigment (pH 7) was bleached in the spectrophotometer for 5 s after recording a dark spectrum. Subsequently, spectra were continuously recorded, and aliquots were removed at defined time points. Part of the aliquot was used in the filter-binding assay to determine the transducin activation rate. The rest of the aliquot was acid-denatured to convert all remaining Schiff base containing pigments into a 440 nm absorbing form. The contribution of the 382 nm pigment to the composite absorbance of photoproduct and free *all-trans*-retinal at 382 nm could thereby be estimated. Figure 6A shows the spectral changes occurring during the time course of the experiment at pH 7. The thermal conversion of the 474 nm photoproduct to the 382 nm photoproduct was essentially complete after 60 min. In the same time range, the rate of transducin activation by the photoproduct mixture decayed in parallel by 92% of its initial value (Figure 6B). The major loss of transducin activation occurred with the transition of the 474 nm species to the 382 nm form, suggesting that transducin activation was mainly due to the 474 nm species. However, not all of the 382 nm absorbance was attributable to the 382 nm mutant photoproduct. The acid denaturation data presented in Figure 6C show that after 60 min about 90% of the pigment Schiff base was already hydrolyzed. These data indicate that the 382 nm photoproduct may not be a prerequisite for transducin activation by E113A/A117E.

Since exact values for the absorption coefficients of the 474 nm and the 382 nm species are not known, the relative absorption at these wavelengths cannot be translated into relative concentrations even if the absorbance of free *all-trans*-retinal can be taken into account. The straightforward interpretation of the similar time dependence of the 474 nm absorption loss and the decay of transducin activation at pH 7 would not be adequate in the case where considerable differences existed between molar extinctions of the photoproducts. Therefore, conditions were chosen where the Schiff base hydrolysis was slow relative to the 474 nm to 382 nm photoproduct conversion. In such a case, the 1:1 stoichiometry of the photoproduct transition (474 nm species to 382 nm species) would allow a direct measurement of the relative amounts of the photoproduct forms since only two components make up the mixture. The data in Figure 5 show that the 474 nm to 382 nm conversion was the most rapid at pH 8. Although the interactions with transducin were weaker at this pH (lower activation rates as shown by Figure 4 and less pronounced stabilization of 474 nm form as shown in Figure 5), a repetition of the experiment in Figure 6 at more alkaline pH was required to correlate the time-dependent spectral changes with the change in transducin activation rates before Schiff base hydrolysis would significantly affect the total amount of pigment present.

Figure 7 shows the results of simultaneous measurements of UV–visible absorption (A), transducin activation (B), and acid denaturation (C) at pH 8. As expected, the 474 nm form was converted to a 382 nm species almost completely in 10 min (Figure 7A). However, as was the case in the pH 7 experiment, the loss of transducin activation occurred again in parallel with the 474 nm absorption decrease (Figure 7B). Importantly, the amount of Schiff base changed only by 8% over 10 min (Figure 7C). This clearly demonstrated that the 382 nm photoproduct containing a covalently bound chromophore accumulated during the first 10 min of the experiment whereas in the same period the transducin activation rate declined.

In a control experiment, the residual transducin activation rate 10 min after photoactivation of the mutant was compared to the noncatalytic nucleotide exchange by transducin in the absence of pigment. Figure 8 shows that the 382 nm form mainly present after this decay time barely activated transducin, as shown by a residual level not significantly different from noncatalytic nucleotide exchange. In contrast, the relative amount of the 474 nm form correlated well with the transducin activation rates measured over 30 min. Figure 9 shows a direct positive linear relationship between the transducin activation rate and the amount of 474 nm photoproduct. We conclude that the formation of the 382 nm photoproduct is not a prerequisite for transducin activation by the mutant E113A/A117E.

DISCUSSION

In mutant E113A/A117E, the endogenous Schiff base counterion was repositioned by one helix turn distal to the original site (Figure 1). The mutant was designed so that the

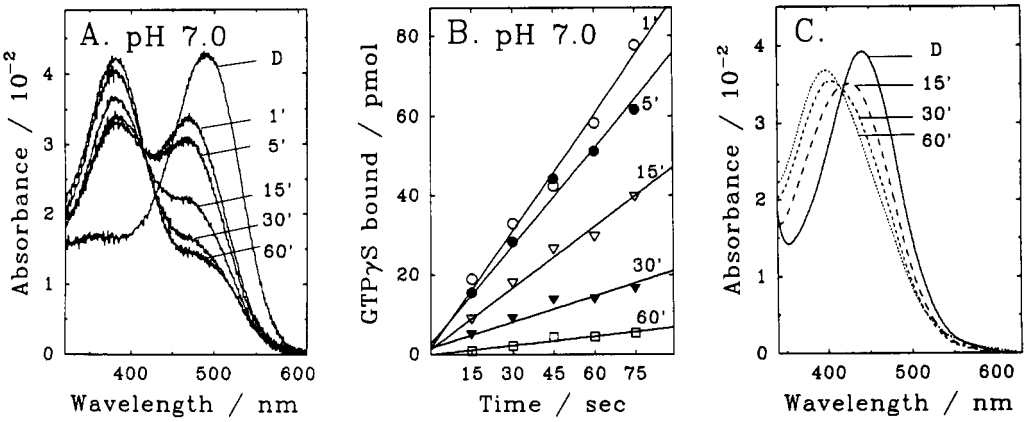

FIGURE 6: Comparison of the thermal decay rate of the 474 nm mutant photoproduct, the decay of transducin activation by mutant E113A/A117E, and Schiff base hydrolysis at pH 7. (A) A pigment sample was illuminated at pH 7.0 to produce the typical mixture of 474 nm and 382 nm absorbing species. The sample was then incubated in the dark at 15 °C, and spectra were recorded at regular time intervals to monitor the thermal conversion from 474 nm to 382 nm peaks. Spectra are shown superimposed for 1, 5, 15, 30, and 60 min after illumination. (B) Aliquots of the sample described in panel A were removed at regular time intervals and subjected to a filter-binding assay to measure the transducin activation rate. The amount of GTPγS bound to the nitrocellulose filter is plotted as a function of time. The time (relative to the photoactivation) at which the aliquot was subjected to the assay is indicated at the end of the regression lines drawn through the data points. (C) The decrease in the amount of Schiff base present in the photolyzed mutant sample was measured in parallel by acid denaturation.

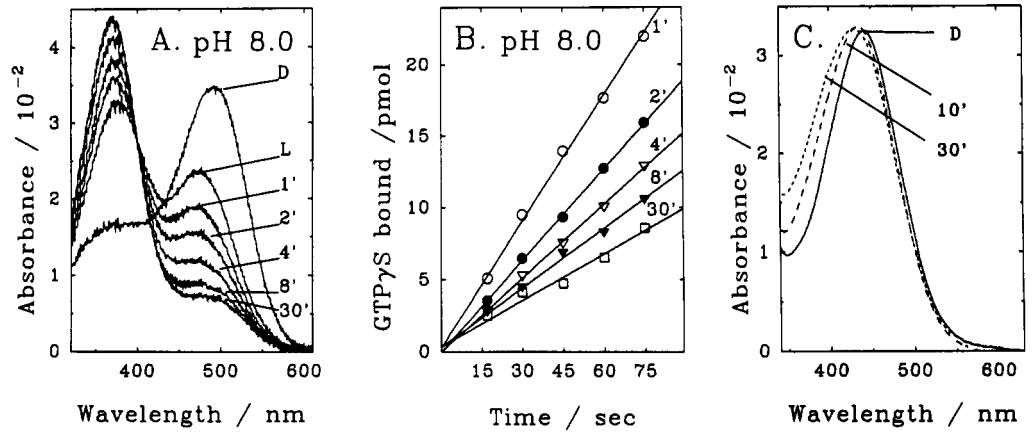

FIGURE 7: Comparison of the thermal decay rate of the 474 nm mutant photoproduct, the decay of transducin activation by mutant E113A/A117E, and Schiff base hydrolysis at pH 8. Conditions were as described in the legend to Figure 6 except that the pH was adjusted to 8 and filter-binding assays were performed at shorter time intervals. (A) A pigment sample was illuminated at pH 8.0 to produce the typical mixture of 474 nm and 382 nm absorbing species. The sample was then incubated in the dark at 15 °C, and spectra were recorded at regular time intervals to monitor the thermal conversion from 474 nm to 382 nm peaks. Spectra are shown superimposed for 1, 2, 4, 8, and 30 min after illumination. (B) Aliquots of the sample described in panel A were removed at regular time intervals and subjected to a filter-binding assay to measure the transducin activation rate. The amount of GTPγS bound to the nitrocellulose filter is plotted as a function of time. The time (relative to the photoactivation) at which the aliquot was subjected to the assay is indicated at the end of the regression lines drawn through the data points. (C) The decay of the amount of Schiff base present in the photolyzed mutant sample was measured in parallel by acid denaturation. Note that the 474 nm to 382 nm absorption shift proceeded faster than at pH 7, whereas the Schiff base decay was slowed down at pH 8. Consequently, a larger amount of the 382 nm photoproduct containing a Schiff base linkage accumulated at pH 8 as compared to pH 7.

putative Schiff base proton acceptor, Glu^{113} (Fahmy et al., 1993), was removed while retaining a carboxylate group in the vicinity of the Schiff base so that the dark-state Schiff base pK_a would be unaffected. Photoactivation of the mutant opsin regenerated with 11-*cis*-retinal (λ_{max} = 491 nm) created a mixture of two photoproducts absorbing at 382 and 474 nm. At acidic pH, the 474 nm species containing a protonated Schiff base was favored, whereas at alkaline pH the 382 nm form indicative of an unprotonated Schiff base was predominant (Figure 2). The Schiff base pK_a of the dark state was not significantly affected. Similar properties have been reported in a study on the mutant E113Q/A117D (Zhukovsky et al., 1992). In spite of the pronounced effect of pH on the relative composition of the photoproduct mixture, no shift in the pH optimum of transducin activation by the mutant was observed (Figure 4). The pH dependence of complex formation between the mutant R* and transducin and the subsequent nucleotide exchange did not differ significantly from those of rhodopsin.

However, a direct interaction between the 474 nm absorbing mutant photoproduct and transducin was demonstrated by a series of experiments discussed below. At any pH, a slow transition from the 474 nm to the 382 nm absorbing form was observed (Figure 5). It was shown that transducin binding stabilized the thermal conversion of the 474 nm photoproduct to a 382 nm species (Figure 5, Table 1). Since excess GTPγS abolished the transducin stabilization of the 474 nm form, the complexes between the 474 nm form and transducin were capable of undergoing nucleotide-dependent dissociation. A simultaneous measurement of spectral changes, transducin activation, and Schiff base decay demonstrated the catalytic activation of transducin by the 474 nm mutant photoproduct (Figures 6 and 7). In particular, at pH 8 transducin activation proceeded almost exclusively via the 474 nm species even

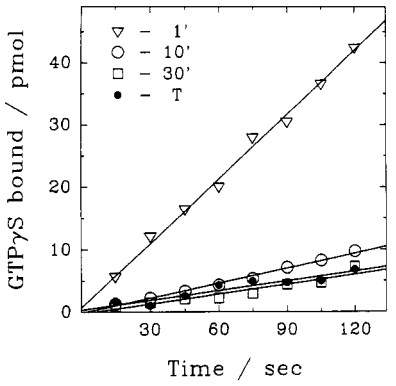

FIGURE 8: Time course of the GTPγS filter-binding assay at pH 8. The fast decay of transducin activation by the thermally reacting photoproduct mixture (Figure 7) was reproduced in this independent experiment. In addition, noncatalytic nucleotide exchange was measured at the end of the experiment to show that activity decay was complete by 30 min. Conditions are as described in the legend to Figure 7.

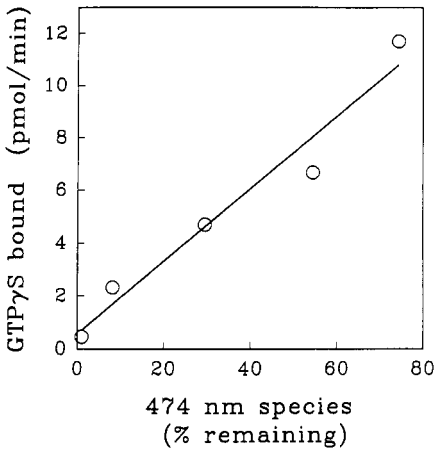

FIGURE 9: Correlation between the amount of the 474-nm absorbing photoproduct of mutant E113A/A117E and the rate of transducin activation at pH 8. The slopes of the regression lines shown in Figure 7B are plotted as a function of the 474 nm absorbance measured at the time after photoactivation at which the filter binding assay was started. A linear regression was drawn through the data to demonstrate the direct positive linear relation between transducin activation and the amount of 474 nm species (relative to that measured directly after illumination of the sample).

though a large amount of 382 nm form accumulated under these conditions (Figure 7A) since Schiff base decay was slow (Figure 7C).

The light-activated form of mutant E113A/A117E apparently contained a protonated Schiff base linkage. The possibility of transducin activation by a recombinant rhodopsin photoproduct containing a protonated Schiff base has also been suggested recently for the mutant G90D (Rao et al., 1994). Likewise, in a study of native rhodopsin regenerated with 11-*cis*-9-desmethylretinal, weak transducin activation was observed in spite of the fact that no Schiff base deprotonation was observed in this pigment, although the possibility of minute amounts of residual native pigment could not be ruled out (Ganter et al., 1989).

In native rhodopsin, deprotonation of the retinylidene Schiff base linkage occurs rapidly after photoisomerization of the chromophore to the all-trans form. Schiff base deprotonation is considered to be a crucial step to switch from an inactive to an active receptor conformation. It has been shown that a chemically modified rhodopsin in which a permanent positive charge was introduced at the Schiff base by methylation failed to form R* and activate transducin (Longstaff et al., 1986). However, recent studies of a rhodopsin mutant, E113Q, in which the Schiff base pK_a was markedly reduced showed that the mutant opsin regenerated with *all-trans*-retinal was able to activate transducin in the dark (Sakmar et al., 1989). Moreover, further study of the same mutant revealed that 11-cis to all-trans isomerization of the retinal chromophore could produce an active R* conformation of the mutant irrespective of the initial protonation state of the Schiff base (Fahmy & Sakmar, 1993b). On the basis of these observations, it was suggested that an all-trans chromophore and a neutral residue at position 113 may be minimal requirements for the conformation of R*. It has also been proposed that the Schiff base deprotonation in rhodopsin may provide the mechanism for light-dependent neutralization of Glu^{113} by coupling proton movement to the thermal reactions subsequent to photoisomerization of the chromophore (Fahmy et al., 1993). These findings concerning the receptor active state generally agree with the constitutive activity found in mutants in which an electrostatic interaction between Lys^{296} and Glu^{113} was abolished by mutations of either residue (Cohen et al., 1992, 1993; Robinson et al., 1992).

The suggested neutralization of Glu^{113} in rhodopsin via Schiff base deprotonation would appear to be a necessary step in receptor activation and is consistent with results obtained with a chemically modified rhodopsin in which a permanently positively charged methylated Schiff base linkage was introduced (Longstaff et al., 1986). This chemically modified pigment may allow Glu^{113} to remain ionized even after photoisomerization and prohibit an active receptor conformation despite the presence of an *all-trans*-retinal chromophore in the binding pocket.

In the case of both mutants E113Q and E113A/A117E, the carboxylate at position 113 is replaced by a neutral residue by mutagenesis. Although the protonation states of Glu^{117} in the double mutant photoproducts are not known directly from the present work, it is clear that net Schiff base deprotonation is not essential for mutant R* conformation. Since the time scale of the present experiments cannot rule out a transient Schiff base deprotonation, the 474 nm species may be thought of as either an active MI-like photoproduct or a reprotonated MII-like photoproduct. However, conformational similarities between the native MII state and the conformation of the 474 nm mutant photoproduct are anticipated and will be evaluated in future experiments. For example, preliminary Fourier-transform infrared (FTIR) spectroscopy data on the mutant E113A/A117E show that the formation of the 474 nm mutant photoproduct is accompanied by infrared absorption changes similar to those observed during the rhodopsin to MII transition (Fahmy et al., unpublished results). These studies also indicate that 11-cis to all-trans isomerization occurred to produce the 474 nm mutant photoproduct.

The salient results of this study are consistent with transducin activation by a rhodopsin mutant containing a protonated Schiff base in the light-activated state. The mutations at positions 113 and 117 provide suitable backgrounds for other mutations which modulate the environment of the Schiff base proton in order to further evaluate its role in the photoactivation mechanism.

ACKNOWLEDGMENT

We thank K. P. Hofmann, O. Ernst, C. Min, and R. Franke for helpful discussions, and J. Dougherty of the RU Instrument Shop.

REFERENCES

Bennett, N., Michel-Villaz, M., & Kühn, H. (1982) *Eur. J. Biochem. 127*, 96–103.

Bownds, D. (1967) *Nature 216*, 1178–1181.

Bruckert, F., Chabre, M., & Vuong, T. M. (1992) *Biophys. J. 63*, 616–629.

Chan, T., Lee, M., & Sakmar, T. P. (1992) *J. Biol. Chem. 267*, 9478–9480.

Cohen, G. B., Oprian, D. D., & Robinson, P. R. (1992) *Biochemistry 31*, 12592–12601.

Cohen, G. B., Yang, T., Robinson, P. R., & Oprian, D. D. (1993) *Biochemistry 32*, 611–615.

Doukas, A. G., Aton, B., Callender, R. H., & Ebrey, T. G. (1978) *Biochemistry 17*, 2430–2435.

Dratz, E. A., & Hargrave, P. A. (1983) *Trends Biochem. Sci. 8*, 128–131.

Emeis, D., Kühn, H., Reichert, J., & Hofmann, K. P. (1982) *FEBS Lett. 143*, 29–34.

Fahmy, K., & Sakmar, T. P. (1993a) *Biochemistry 32*, 7229–7236.

Fahmy, K., & Sakmar, T. P. (1993b) *Biochemistry 32*, 9165–9171.

Fahmy, K., Jaeger, F., Beck, M., Zvyaga, T., Sakmar, T. P., & Siebert, F. (1993) *Proc. Natl. Acad. Sci. U.S.A. 90*, 10206–10210.

Faurobert, E., Otto-Bruc, A., Chardin, P., & Chabre, M. (1993) *EMBO J. 12*, 4191–4198.

Ferretti, L., Karnik, S. S., Khorana, H. G., Nassal, M., & Oprian, D. D. (1986) *Proc. Natl. Acad. Sci. U.S.A. 83*, 599–603.

Franke, R. R., Sakmar, T. P., Oprian, D. D., & Khorana, H. G. (1988) *J. Biol. Chem. 263*, 2119–2122.

Franke, R. R., König, B., Sakmar, T. P., Khorana, H. G., & Hofmann, K. P. (1990) *Science 250*, 123–125.

Franke, R. R., Sakmar, T. P., Graham, R. M., & Khorana, H. G. (1992) *J. Biol. Chem. 267*, 14767–14774.

Fung, B. K.-K., Hurley, J. B., & Stryer, L. (1981) *Proc. Natl. Acad. Sci. U.S.A. 75*, 152–156.

Ganter, U. M., Schmid, E. D., Perez-Sala, D., Rando, R. R., & Siebert, F. (1989) *Biochemistry 28*, 5954–5962.

Hofmann, K. P. (1986) *Photobiochem. Photobiophys. 13*, 309–338.

Honig, B., Greenberg, A. D., Dinur, U., & Ebrey, T. G. (1976) *Biochemistry 15*, 4593–4599.

Honig, B., Ebrey, T. G., Callender, R. H., Dinur, U., & Ottolenghi, M. (1979) *Proc. Natl. Acad. Sci. U.S.A. 76*, 2503–2507.

Irving, C. S., Byers, G. W., & Leermakers, P. A. (1969) *J. Am. Chem. Soc. 91*, 2141–2143.

Irving, C. S., Byers, G. W., & Leermakers, P. A. (1970) *Biochemistry 9*, 858–864.

Karnik, S. S., Sakmar, T. P., Chen, H.-B., & Khorana, H. G. (1988) *Proc. Natl. Acad. Sci. U.S.A. 85*, 8459–8463.

Kibelbek, J., Mitchell, D. C., Beach, J. M., & Litman, B. L. (1991) *Biochemistry 30*, 6761–6768.

Kropf, A., & Hubbard, R. (1958) *Ann. N.Y. Acad. Sci. 74*, 266–280.

Lin, S. W., Sakmar, T. P., Franke, R. R., Khorana, H. G., & Mathies, R. A. (1992) *Biochemistry 31*, 5105–5111.

Longstaff, C., Calhoon, R. D., & Rando, R. R. (1986) *Proc. Natl. Acad. Sci. U.S.A. 83*, 4209–4213.

Mathews, R. G., Hubbard, R., Brown, P. K., & Wald, G. (1963) *J. Gen. Physiol. 47*, 215–240.

Nathans, J. (1990) *Biochemistry 29*, 9746–9752.

Oprian, D. D., Molday, R. S., Kaufman, R. J., & Khorana, H. G. (1987) *Proc. Natl. Acad. Sci. U.S.A. 84*, 8874–8878.

Oseroff, A. R., & Callender, R. H. (1974) *Biochemistry 13*, 4243–4348.

Parkes, J., & Liebman, P. A. (1984) *Biochemistry 23*, 5054–5061.

Rao, V. R., Cohen, G. B., & Oprian, D. D. (1994) *Nature 367*, 639–642.

Robinson, P. R., Cohen, G. B., Zhukovsky, E. A., & Oprian, D. D. (1992) *Neuron 9*, 719–725.

Sakmar, T. P., Franke, R. R., & Khorana, H. G. (1989) *Proc. Natl. Acad. Sci. U.S.A. 86*, 8309–8313.

Sakmar, T. P., Franke, R. R., & Khorana, H. G. (1991) *Proc. Natl. Acad. Sci. U.S.A. 88*, 3079–3083.

Weitz, C. J., & Nathans, J. (*1993*) *Biochemistry 32*, 14176–14182.

Wessling-Resnick, M., & Johnson, G. L. (1987) *J. Biol. Chem. 262*, 3697–3705.

Yoshizawa, T., & Shichida, Y. (1982) *Methods Enzymol. 8*, 333–354.

Zhukovsky, E. A., & Oprian, D. D. (1989) *Science 246*, 928–930.

Zhukovsky, E. A., Robinson, P. R., & Oprian, D. D. (1992) *Biochemistry 31*, 10400–10405.

Zvyaga, T. A., Min, K. C., Beck, M., & Sakmar, T. P. (1994) *J. Biol. Chem. 269*, 13056.